

ChREBP-driven DNL and PNPLA3 Expression Induced by Liquid Fructose are Essential in the Production of Fatty Liver and Hypertriglyceridemia in a High-Fat Diet-Fed Rat Model

Ana Magdalena Velázquez, Roger Bentanachs, Aleix Sala-Vila, Iolanda Lázaro, Jose Rodríguez-Morató, Rosa M. Sánchez, Marta Alegret, Núria Roglans,* and Juan Carlos Laguna*

Scope: The aim of this study is to delineate the contribution of dietary saturated fatty acids (FA) versus liquid fructose to fatty liver and hypertriglyceridemia.

Methods and Results: Three groups of female rats are maintained for 3 months in standard chow (CT); High-fat diet (46.9% of fat-derived calories, rich in palmitic and stearic FA, HFD); and HFD with 10% w/v fructose in drinking water (HFHFr). Zoometric parameters, plasma biochemistry, and liver Oil-Red O (ORO) staining, lipidomics, and expression of proteins involved in FA metabolism are analyzed. Both diets increase ingested calories without modifying body weight. Only the HFHFr diet increases liver triglycerides (x11.0), with hypertriglyceridemia (x1.7) and reduces FA β -oxidation (x0.7), and increases liver FA markers of DNL (de novo lipogenesis). Whereas HFD livers show a high content of ceramides, HFHFr samples show unchanged ceramides, and an increase in diacylglycerols. Only the HFHFr diet leads to a marked increase in the expression of enzymes involved in DNL and triglyceride metabolism, such as carbohydrate response element binding protein β (ChREBP β , x3.2), a transcription factor that regulates DNL, and patatin-like phospholipase domain-containing 3 (PNPLA3, x2.6), a lipase that mobilizes stored triglycerides for VLDL secretion.

Conclusion: The addition of liquid-fructose to dietary FA is determinant in liver steatosis and hypertriglyceridemia production, through increased DNL and PNPLA3 expression, and reduced FA catabolism.

1. Introduction

NAFLD (non-alcoholic fatty liver disease) currently affects 25% of the human population, with its prevalence on the rise. At least a quarter of this population will evolve from simple steatosis to NASH (steatohepatitis), increasing the risk of liver fibrosis and cirrhosis. Liver steatosis or fatty liver is reversible and involves the accumulation of TG (triglycerides) in the form of lipid droplets in at least 5% of the hepatocytes.^[1] NAFLD, either in the form of fatty liver or NASH/cirrhosis, is a risk factor for hepatocellular carcinoma.^[2] Although fatty liver can be theoretically prevented or treated effectively by changes in lifestyle through addressing dietary habits and physical activity, these changes are difficult to maintain over time.^[3] Unfortunately, there is no approved drug therapy for NAFLD, and there is an urgent need to fill this void therapeutic niche.^[4] To this end, experimental animal models

A. M. Velázquez, R. Bentanachs, R. M. Sánchez, M. Alegret, N. Roglans, J. C. Laguna
 Department of Pharmacology, Toxicology and Therapeutic Chemistry,
 School of Pharmacy and Food Science
 University of Barcelona
 Avda Joan XXIII 27–31, Barcelona 08028, Spain
 E-mail: roglans@ub.es; jclagunae@ub.edu


R. M. Sánchez, M. Alegret, N. Roglans, J. C. Laguna
 Institute of Biomedicine
 University of Barcelona
 Barcelona 08028, Spain

J. Rodríguez-Morató, R. M. Sánchez, M. Alegret, N. Roglans, J. C. Laguna
 Spanish Biomedical Research Centre in Physiopathology of Obesity and
 Nutrition (CIBEROBN)
 Instituto de Salud Carlos III (ISCIII)
 Madrid 28029, Spain

A. Sala-Vila, I. Lázaro, J. Rodríguez-Morató
 IMIM-Hospital del Mar Medical Research Institute
 Barcelona 08003, Spain

A. Sala-Vila
 Barcelona β eta Brain Research Center
 Pasqual Maragall Foundation
 Barcelona 08005, Spain

J. Rodríguez-Morató
 Department of Experimental and Health Sciences
 Universitat Pompeu Fabra (CEXS-UPF)
 Barcelona 08003, Spain

 The ORCID identification number(s) for the author(s) of this article can be found under <https://doi.org/10.1002/mnfr.202101115>

© 2022 The Authors. Molecular Nutrition & Food Research published by Wiley-VCH GmbH. This is an open access article under the terms of the Creative Commons Attribution-NonCommercial License, which permits use, distribution and reproduction in any medium, provided the original work is properly cited and is not used for commercial purposes.

DOI: 10.1002/mnfr.202101115

of NAFLD, mainly rodent models, are essential for research of new therapeutic approaches.

The fatty acids associated with liver-related lipid metabolism are, in normal circumstances, provided by the diet, with a small contribution from DNL (de novo lipogenesis), which accounts for no more than 5% of the total pool of fatty acids.^[5] Despite that, one consistent characteristic found in livers of NAFLD patients is that DNL contributes up to 30% of the pool of fatty acids that are processed.^[5]

Among experimental animal models of NAFLD, dietary models mimicking unhealthy dietary patterns in humans, such as the Western hypercaloric diet that is rich in saturated fat and simple sugars, are the most useful.^[6] However, these models have several drawbacks, including the lengthy periods of time needed to achieve the desired liver pathophysiological changes, difficulties in establishing a clear-cut separation between a simple fatty liver and steatohepatitis, and the concomitant appearance of comorbidities such as obesity or insulin resistance/type 2 diabetes that makes it difficult to ascertain if the liver pathology is an independent entity or a consequence of the associated metabolic disturbance. The use of palmitic acid (16:0), a saturated fatty acid with a high pro-inflammatory potential,^[7] as almost the sole dietary fat source, as well as other factors as the presence of dietary cholesterol or high proportions of fructose/sucrose incorporated into solid diets, favoring the early promotion of a liver inflammatory process, could be at the basis of these drawbacks, especially regarding the difficulty to clearly dissociate the appearance of steatohepatitis from fatty liver.

Based on our previous experience of studying the effects of liquid fructose supplementation in Sprague-Dawley female rats,^[8–12] we have developed a dietary rat model of fatty liver that addresses the above mentioned drawbacks. To do so, we administered to Sprague-Dawley female rats a high-fat solid diet, supplemented with a solution of liquid fructose as the beverage, for three months. To avoid a pro-inflammatory effect of the diet, we used a solid diet: i) enriched in palmitic acid together with stearic acid (18:0), a saturated fatty acid that is metabolized to oleic acid (18:1),^[13,14] to counteract the pro-inflammatory effect of palmitic acid;^[15] (ii) devoid of dietary cholesterol, which is known to promote liver inflammation;^[16] and (iii) supplemented with liquid fructose at a low concentration to minimize gut inflammation and the consequent leaking of pro-inflammatory bacterial toxins into the portal circulation.^[10] Here, we present data showing that compared with the high-fat solid diet, the addition of liquid fructose supplementation led to the appearance of histological and biochemical signs of fatty liver, hypertriglyceridemia, and early signs of insulin resistance, without increases in white adipose tissue and body weight as well as in the levels of liver inflammatory markers. Thus, in a relatively short time (three months), we reproduced in our model the earliest manifestation of NAFLD, fatty liver, independently of other metabolic disturbances, such as obesity, liver inflammation, or established type 2 diabetes mellitus. Furthermore, we present biochemical, gene expression (mRNA and protein), and lipidomic data from this model, showing the relevance of fructose-induced alterations in hepatic lipid homeostasis in the development of these pathological changes.

2. Results

2.1. No Dietary Intervention Induced Significant Changes in Body Weight and Liver Inflammation

Consumption of the HFD rich in palmitic and stearic resulted in a significant increase (x1.24) in the ingested total calories with respect to control rats. This increase was even larger when liquid fructose was added to the solid diet (x1.62, 49.8% of total calories provided by fructose, equivalent to 2948±507 kcal 90 days⁻¹ rat⁻¹) (Figure 1A). However, total body weight (Figure 1B1) and the weight of the sWAT and pWAT (Figure 1B2) were not modified at the end of the dietary interventions. Only liver weight was significantly increased (x1.20) in the HFHFr dietary group (Figure 1B3). We have previously shown that the HFHFr dietary intervention does not affect the locomotor activity of rats in an open field test,^[17] precluding an increased rate of calorie burning due to increased muscular activity. Instead, we found that both dietary interventions increased the protein levels of β_3 -AR (β_3 -adrenergic receptor, x1.7 and x1.6 for HFD and HFHFr, respectively), and UCP1 (uncoupling protein 1, x2.7 and x3.9 for HFD and HFHFr, respectively), as well as PGC-1 α (peroxisome proliferator activated receptor- γ coactivator-1 α) in the case of HFHFr rats (x1.8), in the BAT samples (Figure 1C). Thus, the lack of an increase in body weight associated with a high caloric intake can be attributed to increased thermogenic activity in BAT produced by the HFD and HFHFr interventions.

Although the livers were enlarged, at least in HFHFr-treated rats, no sign of liver necrosis could be observed in the analysis of haematoxylin-eosin-stained liver samples (Figure 1D) from the dietary groups compared with controls. Moreover, no increase in serum alanine and aspartate aminotransferase concentrations was observed (Figure 1E), as there were also no increases in the liver expression of markers of oxidative stress (catalase, glutathione peroxidase 1, and superoxide dismutase 2) and inflammation (tumour necrosis factor α , and F4/80) (Figure 1F). In accordance with the lack of changes in the liver inflammatory markers and with the liver pro-inflammatory activity of dietary cholesterol, no changes in the liver cholesterol concentration were observed (Figure 1G).

Another possible effect of an excessive consumption of hyper-caloric diets is the induction of endoplasmic reticulum stress.^[18,19] In the liver samples, only the HFHFr diet significantly increased (x5.0) the phosphorylation of IRE-1 (inositol-requiring enzyme-1) at Ser⁷²⁴ (Figure 2A), while reducing the amount of phosphorylated (x0.5) (at Thr⁹⁸¹) and total (x0.5) PERK (protein kinase RNA-like endoplasmic reticulum kinase) (Figure 2B), without significantly affecting the expression of the precursor and mature forms of ATF6 (activating transcription factor 6) (Figure 2C). The HFD had no significant effect on these parameters. However, the changes in the protein levels of IRE-1 and PERK in the livers of HFHFr rats did not translate in any significant changes in the expression of the markers of their respective signaling pathways (Figure 2D).

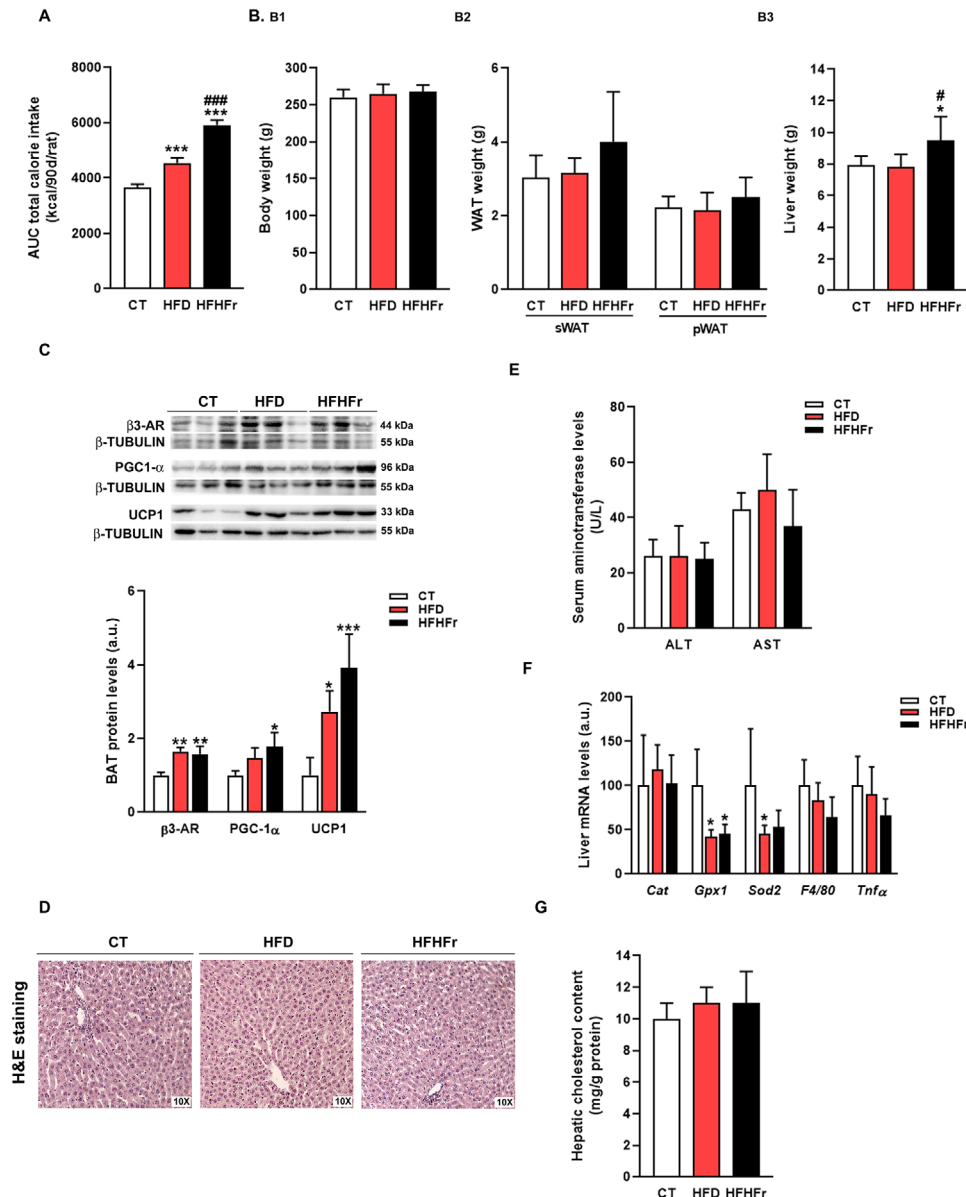


Figure 1. Effect of HFD and HFHFr on caloric intake, body weight, thermogenic markers in BAT, and inflammatory markers in liver: A) Bar plots showing the AUC of caloric intake for the full length of the study (3 months) corresponding to the three experimental groups studied: Control (CT), high fat diet (HFD), and high fat high fructose group (HFHFr) female Sprague-Dawley rats. B) Bar plots showing body weight (B1), subcutaneous (sWAT) and perigonadal (pWAT) weights (B2), and liver weight (B3) at the end of the experimental period corresponding to CT, HFD, and HFHFr rats. C) Bar plots showing the content of β 3-AR, PGC-1 α , and UCP1 proteins in the BAT tissue obtained from CT, HFD, and HFHFr rats (a.u.: arbitrary units); in the upper part of the figure, representative WB bands corresponding to the three different study groups are shown. D) Haematoxylin-Eosin (10x) representative stained liver samples corresponding to CT, HFD, and HFHFr rats. E) Bar plots showing serum levels of ALT and AST of CT, HFD, and HFHFr rats. F) Bar plots showing the relative mRNA levels of *Cat*, *Gpx1*, *Sod2*, *F4/80*, and *Tnfa* genes of liver samples from CT, HFD, and HFHFr rats. G) Bar plots showing the total cholesterol content of liver samples from CT, HFD, and HFHFr rats. Each bar represents the mean \pm SD of 7–8 different samples; for WB analysis, we used three different pooled samples for each experimental condition, each pool was obtained from mixing equal amounts of 2–3 individual tissue samples. *** $p < 0.001$, ** $p < 0.01$, * $p < 0.05$ versus CT; ### $p < 0.001$, # $p < 0.05$ versus HFD.

2.2. Only Rats Consuming the HFHFr Showed Significant Hyperinsulinemia and a Reduced ISI

Neither the HFD nor the HFHFr diet significantly affected the concentrations of blood glucose, serum adiponectin, leptin, and NEFA (non-esterified free fatty acids) with respect to control val-

ues (Figure 3A4, A1-3). Rats fed the HFHFr diet showed increased serum concentrations of insulin (x1.9) (Figure 3A5) compared to control values and, consequently, a significant reduction (x0.7) in the insulin sensitivity index (ISI) (Figure 3A6). In the OGTT (oral glucose tolerance test), blood concentrations of glucose at different times (Figure 3B1) and the AUC (area under

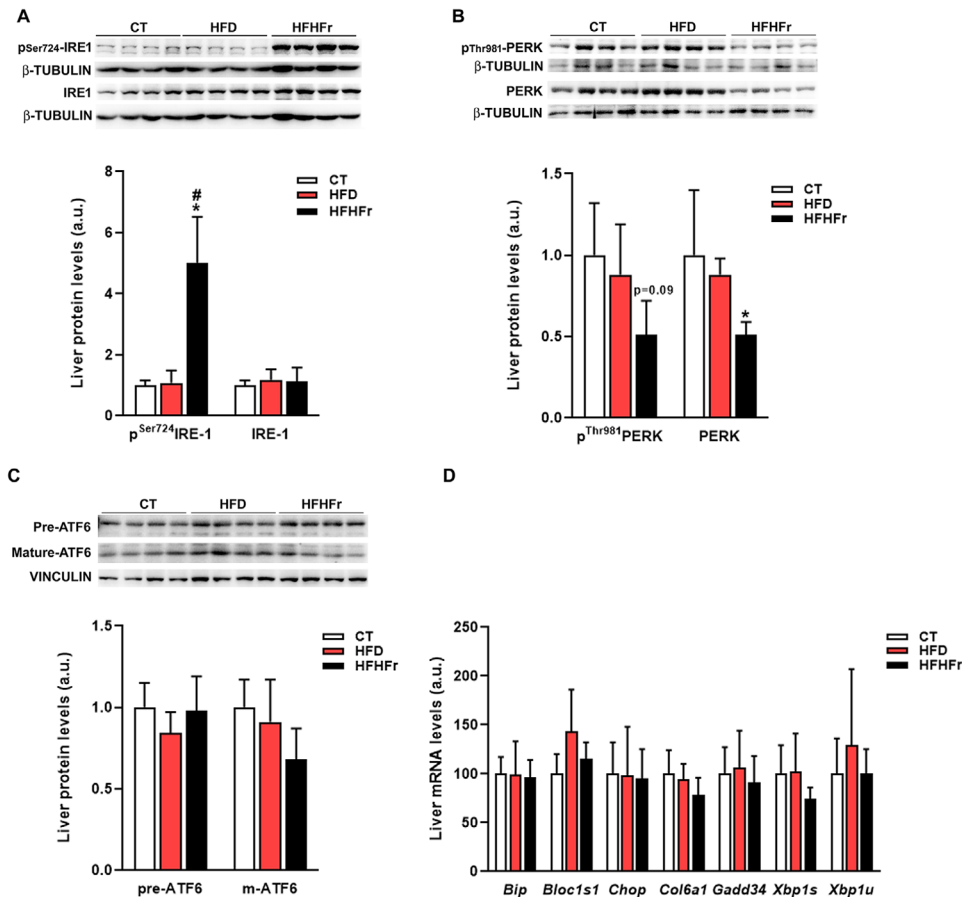


Figure 2. Effect of HFD and HFHFr on liver markers of ER stress: A) Bar plots showing the content of phospho^{Ser724} and total IRE-1 proteins in the liver tissue obtained from CT, HFD, and HFHFr rats (a.u.: arbitrary units); in the upper part of the figure, representative WB bands corresponding to the three different study groups are shown. B) Bar plots showing the content of phospho^{Thr981} and total PERK proteins in the liver tissue obtained from CT, HFD, and HFHFr rats; in the upper part of the figure, representative WB bands corresponding to the three different study groups are shown. C) Bar plots showing the content of the precursor (pre-) and mature (m-) forms of ATF6 proteins in the liver tissue obtained from CT, HFD, and HFHFr rats; in the upper part of the figure, representative WB bands corresponding to the three different study groups are shown. D) Bar plots showing the relative mRNA levels of *Bip*, *Bloc1s1*, *Chop*, *Col6a1*, *Gadd34*, and *Xbp1* (spliced and un-spliced) genes of liver samples from CT, HFD and HFHFr rats. Each bar represents the mean \pm SD of 7–8 different samples; for WB analysis, we used four different pooled samples for each experimental condition, each pool was obtained from mixing equal amounts of two individual liver samples. * $p < 0.05$ versus CT; # $p < 0.05$ versus HFD.

the curve) for glucose concentration (Figure 3B2) were unmodified among the three dietary groups, while insulin concentration showed an earlier and higher peak in the HFHFr group than in controls (Figure 3B3) and there was a nonsignificant increase (x1.3) in the AUC for insulin concentration (Figure 3B4). Overall, only the HFHFr rats showed significant changes in markers suggesting a mild state of whole-body insulin resistance. Given that we observed no changes in WAT weight and serum NEFA concentrations, we examined samples of liver and skeletal muscle tissues from the three groups studied to look for changes in molecular markers of insulin sensitivity.

Accumulation of DAG (diacylglycerol) and Cer (ceramide) species in the liver has been linked to increased liver insulin resistance.^[20,21] Liver samples from the HFD group showed an increased content in Cer species containing long chain saturated fatty acids (stearic, arachidic -20:0- and behenic -22:0- acids), while the content of Cer 24:1 was significantly decreased (x0.60). These changes were completely reverted in samples from the

HFHFr rats, which showed Cer concentrations similar to those of control samples (Figure 3C). On the contrary, the HFHFr liver samples showed significantly increased levels of most of the DAG species analyzed compared with control samples, especially in the case of DAG 16:0 (x4.9), DAG 16:0 18:0 (x7.2), DAG 16:1 (x26.7), DAG 18:0 18:1 (x12.6), DAG 18:1 16:0 (x10.0), and DAG 18:1 (x15.5). The HFD liver samples presented minimal changes in the concentrations of the different DAG species studied, except in the case of DAG 18:0 18:1, which showed a significant increase (x10.6) compared to control values (Figure 3D). When we determined the degree of activation by phosphorylation of several isoforms of PKC (protein kinase C) in the liver samples (Supplemental Figure S1, Supporting Information), a process that has been directly related to DAG accumulation in the liver and to the induction of liver insulin resistance,^[20] the only significant change we found was a decrease (x0.60) in the amount of phospho-PKC μ (Ser916) (also known as PKD^[22]) in the HFHFr liver samples (Figure 3E). Thus, despite significant increases in DAG concen-

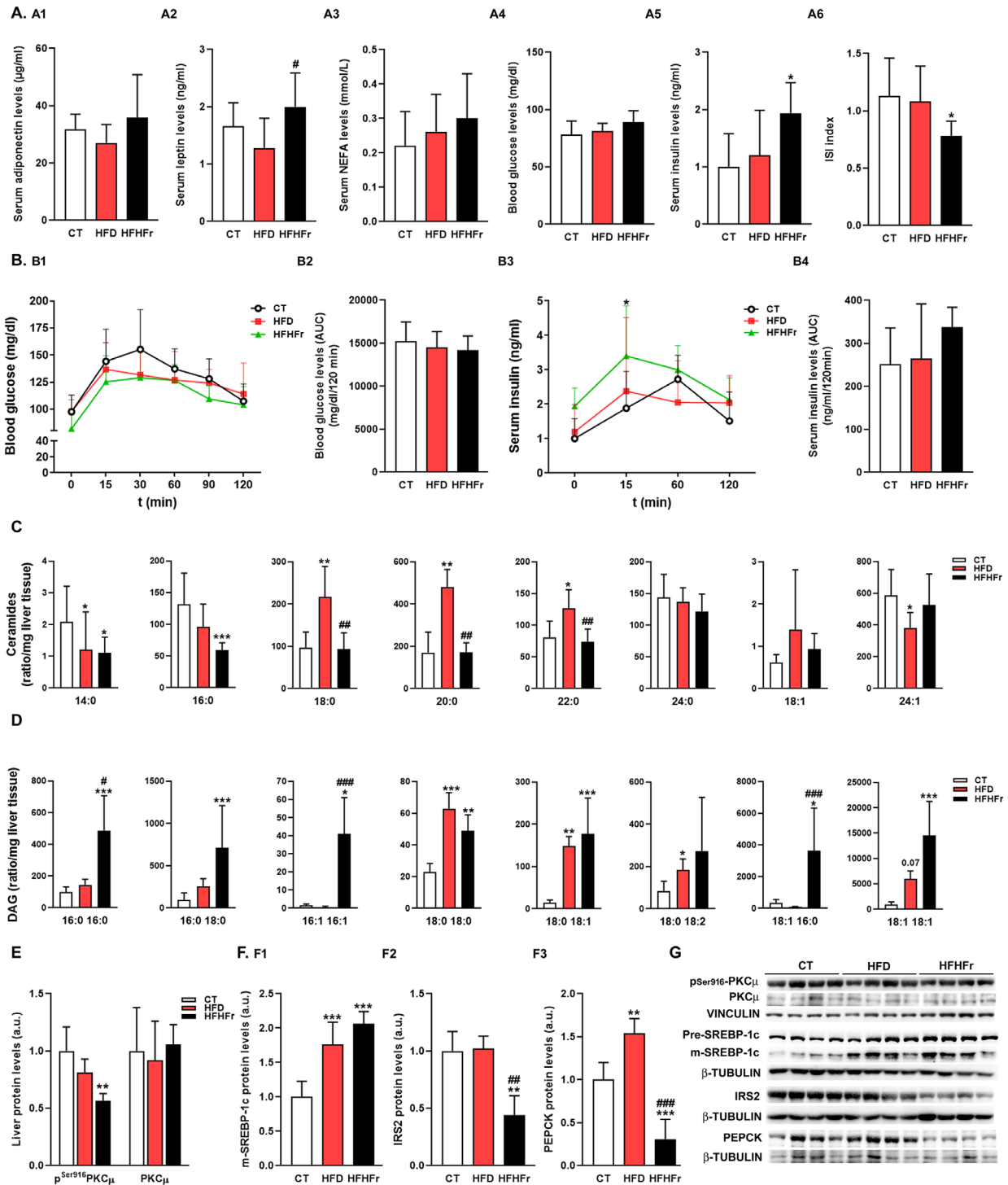


Figure 3. Effect of HFD and HFHFr on several markers of whole body and liver insulin sensitivity: A) Bar plots showing serum levels of adiponectin (A1), leptin (A2), NEFA (A3), and insulin (A5), and blood levels of glucose (A4), as well as the ISI index (A6) of CT, HFD, and HFHFr rats. B) Blood glucose (B1) and serum insulin (B3) values at different times after oral administration of a glucose solution (2 g kg^{-1} body weight), and bar plots showing the corresponding area under the curve (AUC) for glucose (B2) and serum insulin (B4) in CT, HFD, and HFHFr rats. Bar plots showing the levels of (C) ceramides and (D) diacylglycerols (DAG) in rat liver homogenates from CT, HFD, and HFHFr rats. Bar plots showing the content of (E) phospho^{Ser916} and total PKC α proteins, and (F) mature (m-) SREBP1c (F1), IRS2 (F2), and PEPCK (F3) proteins in the liver tissue obtained from CT, HFD, and HFHFr rats (a.u.: arbitrary units); in the right part of the figures (G), representative WB bands corresponding to the three different study groups are shown. Each bar represents the mean \pm SD of 7–8 different samples; for WB analysis, we used four different pooled samples for each experimental condition, each pool was obtained from mixing equal amounts of two individual liver samples. *** $p < 0.001$, ** $p < 0.01$, * $p < 0.05$ versus CT; ### $p < 0.001$, ## $p < 0.01$, # $p < 0.05$ versus HFD.

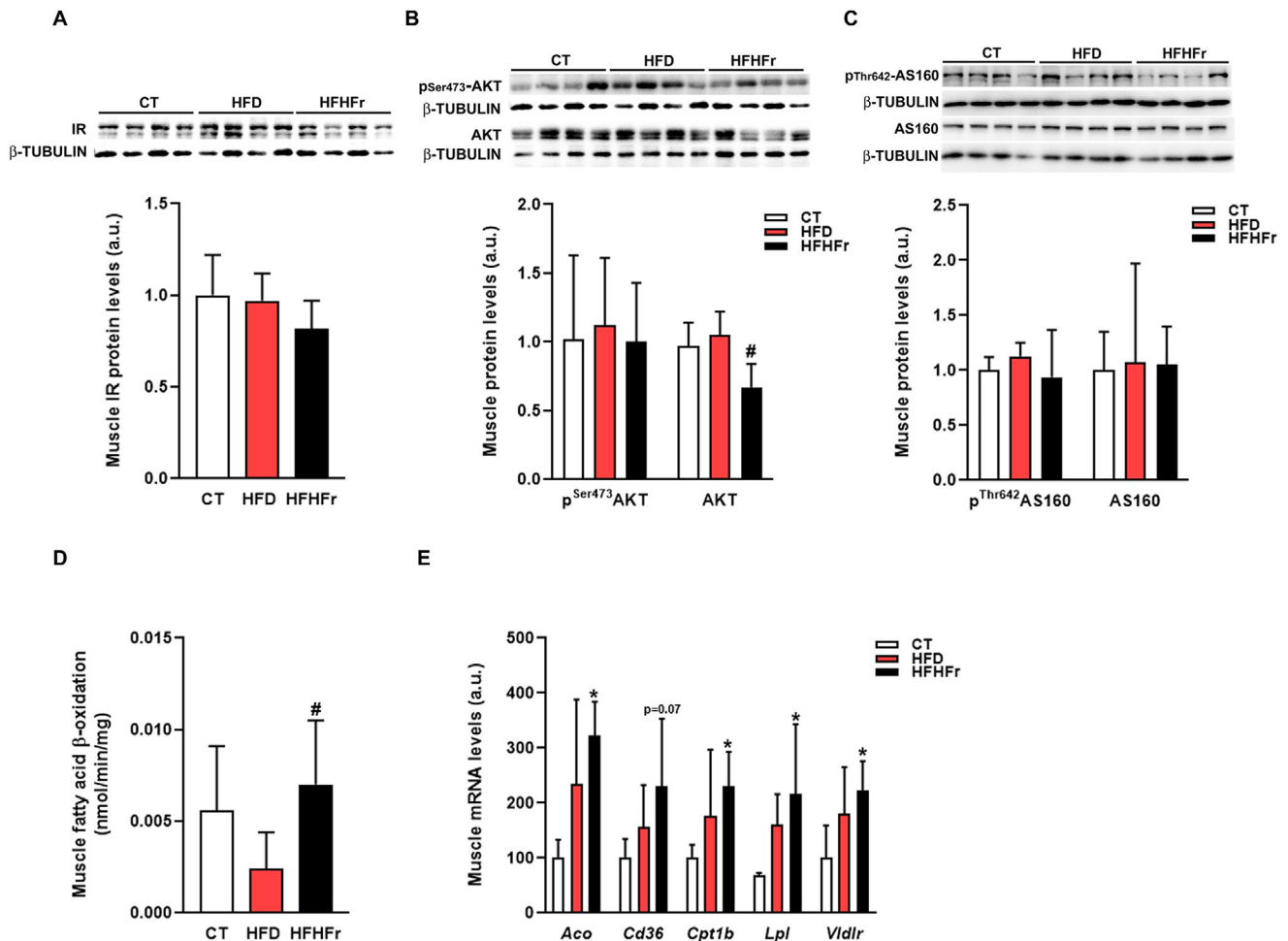


Figure 4. Effect of HFD and HFHFr on several markers of whole body and skeletal muscle insulin sensitivity: Bar plots showing (A) the content of IR, (B) phospho^{Ser473} and total AKT, and (C) phospho^{Thr642} and total AS160 proteins in the muscle tissue obtained from CT, HFD and HFHFr rats (a.u.: arbitrary units); in the upper part of the figures, representative WB bands corresponding to the three different study groups are shown. D) Bar plots showing fatty acid β -oxidation activity and (E) the relative mRNA levels of *Aco*, *Cd36*, *Cpt1b*, *Lpl*, *Gadd34*, and *Vldlr* genes of muscle samples from CT, HFD, and HFHFr rats. Each bar represents the mean \pm SD of 7–8 different samples; for WB analysis, we used four different pooled samples for each experimental condition, each pool was obtained from mixing equal amounts of two individual muscle samples. * $p < 0.05$ versus CT; # $p < 0.05$ versus HFD.

trations in the livers of HFHFr rats, these changes did not result in activation of any of the PKC isoforms studied. In the liver, increased insulin signaling has two main effects: increased activation of SREBP-1c (sterol response element binding protein-1c)-dependent lipogenesis and the suppression of gluconeogenesis. The established consensus is that when liver insulin resistance ensues, the effect of insulin on lipogenesis is maintained, while the suppression of gluconeogenesis disappears, resulting in an increased output of newly synthesized glucose by the liver.^[23] We assessed the expression of several key molecular players of liver insulin signaling. As can be seen in Figure 3F1, the mature form of the SREBP-1c was increased by both dietary interventions (x1.8 and x2.1 for HFD and HFHFr diets, respectively). Moreover, despite a significant reduction (x0.4) in HFHFr liver samples in the expression of the IRS2 (insulin receptor substrate 2) (Figure 3F2), a key transducer of insulin signaling in liver tissue, the expression of the protein PEPCK (phosphoenolpyruvate carboxylase), the rate limiting enzyme in the synthesis of glucose, was

significantly increased by the HFD (x1.5), but decreased (x0.3) by the HFHFr diet (Figure 3F3). We have consistently reported the latter effect of liquid fructose supplementation on PEPCK expression.^[10,12] Overall, these data do not support a clear state of insulin resistance in the livers of rats on the HFD or HFHFr diet.

In the skeletal muscle samples, neither the HFD, nor the HFHFr diet significantly altered the expression of the insulin receptor (Figure 4A), the degree of phosphorylation of the serine/threonine kinase Akt (Figure 4B), and the degree of phosphorylation of AS160 (Akt substrate of 160 kDa)^[24] (Figure 4C). In parallel, fatty acid β -oxidation (Figure 4D) was significantly increased (x1.25) with respect to the values presented by the HFD rats, and there were also increases in the mRNA levels of muscle *lpl* (lipoprotein lipase), *Aco* (acyl-CoA oxidase), *Cpt1b* (carnitine palmitoyl transferase 1b), *Vldlr* (very low density lipoprotein receptor), and *Cd36* (cluster of differentiation *Cd36*, also known as fatty acid translocase) (x3.2, x3.2, x2.3, x2.2, and x2.3 vs

control values, respectively) (Figure 4E). This suggested that muscle metabolism showed increased fatty acid catabolism, probably at the expense of glucose use as an energy fuel.

2.3. Liquid Fructose Supplementation Strongly Affected Liver Fatty Acid Metabolism, Increasing DNL, and Decreasing Fatty Acid β -oxidation Activity, Thereby Resulting in the Development of Fatty Liver and Hypertriglyceridemia

Although the HFD induced a significant increase in liver TG levels, as determined biochemically (x1.6 vs control) and with the ORO histological staining (x1.8 vs control), the induction of fatty liver was highly enhanced by liquid-fructose supplementation (Figure 5A1-3). The HFHFr livers showed a significant accumulation of liver TG (x2.3 vs control) and a huge increase in the ORO-stained surface of histological samples (x11.0) (Figure 5A1-3). This clear state of fatty liver disease was accompanied by the development of significant hypertriglyceridemia (x1.7 vs control) that was not present in the HFD samples (Figure 5B). As there was no significant change in serum NEFA concentrations in the two dietary experimental groups (see Figure 3A3), we investigated the three remaining mechanisms that could be involved in increased liver TG accretion: liver fatty acid catabolism, dietary fatty acids, and liver DNL. Liver fatty acid β -oxidation was significantly reduced (x0.7 vs control, Figure 5C1) in the livers from HFHFr rats, a consistent effect produced by liquid-fructose supplementation^[9,25] that is related mainly to a decreased peroxisomal activity. This was shown by a significant reduction (x0.7 vs control, Figure 5C2) in the expression of the rate-limiting enzyme of peroxisomal fatty acid β -oxidation, ACO (acyl-CoA oxidase), without changes in the expression of L-CPT1 (liver-carnitine palmitoyltransferase 1), the rate limiting enzyme for mitochondrial fatty acid β -oxidation (Figure 5C2). The livers from HFD rats, although presenting a significant increase in the expression of L-CPT1 (x2.3 vs control, Figure 5C2), probably due to an enhanced homeostatic response to the increased amount of dietary fatty acids, showed unmodified total fatty acid β -oxidation activity (Figure 5C1). The analysis of the concentrations of the fatty acids present in liver TG (Figure 5D) indicated that the main change detected in the HFD samples was an increase in the concentration of the two saturated fatty acids provided by the diet, palmitic (x2.6 vs control), and stearic acid (x7.4 vs control). Despite the HFHFr rats consuming less of the solid diet than the HFD rats, the HFHFr liver samples showed a marked increase in the concentration of several fatty acids such as palmitic (x6.3 vs control), stearic (x13.9 vs control), oleic (x17.6 vs control), and especially palmitoleic acid (16:1, x39.2 vs control), pointing to a clear increase in hepatic DNL in these animals. Indeed, the HFHFr diet led to a marked increase in the mRNA (Figure 5E: *Acly* (ATP citrate lyase), *ChREBP α* and β , *Dgat2* (diacylglycerol acyltransferase 2), *Elovl2* and 6 (elongation of very-long fatty acids-like 2 and 6), *Fads2* (fatty acids desaturase 2), *Fas* (fatty acid synthase), *L-pk* (liver-pyruvate kinase), *Plin2* (perilipin 2), *Scd1* (stearoyl-CoA desaturase 1), and *Pnpla3*) and protein (Figure 5F: ACLY, ChREBP α and β , FAS, PNPLA3) levels of several enzymes and proteins involved in fatty acid synthesis and TG deposition and mobilization, as well as in the expression of carbohydrate response element binding protein β (ChREBP β , x3.2), a transcription factor

activated by simple sugars consumption that regulates, among other processes, DNL.^[26] These changes were practically not detected in the liver samples from HFD rats. The expression of the *Mttp* (microsomal triglyceride transfer protein), *Vldlr*, and *ApoC-III* (apolipoprotein CIII) genes was not modified by the two dietary interventions (data not shown). Moreover, the expression of the PNPLA3 gene, a target gene for ChREBP trans-activating activity^[27] that encodes a lipase that mobilizes monounsaturated fatty acid-enriched TG stored in lipid droplets for VLDL formation and secretion,^[28] was significantly increased solely in the HFHFr livers (x29.2 and x2.6 vs control for mRNA and protein, respectively), directly linking fructose-mediated ChREBP activation to the appearance of not only fatty liver, but also hypertriglyceridemia.

3. Discussion

In the present work, we provide experimental data highlighting the key contribution of fructose to changes in liver fatty acid anabolism and catabolism in the development of fatty liver when supplemented on top of a solid high fat diet (46.9% calories) rich in palmitic and stearic acid. Moreover, the activation of the ChREBP pathway in the liver by fructose not only increased DNL, but also led to hypertriglyceridemia through PNPLA3, increasing the flux of fatty acids to the skeletal muscle, thus resulting in signs of insulin resistance in this tissue. In our experimental rat model, these changes were promoted without any manifestation of liver inflammation and no significant changes in total body weight and white adipose tissue weight, despite the significant increase in calorie consumption in both dietary interventions (HFD and HFHFr).

In 1979, Rothwell and Stock first described BAT (brown adipose tissue)-driven diet-induced adaptive thermogenesis associated with the consumption of high calorie diets.^[29] Indeed, in our experimental conditions, both diets increased the expression of markers of thermogenic activity in BAT (see Figure 1C), without significantly changing their expression in sWAT (subcutaneous white adipose tissue) or pWAT (perigonadalWAT) (supplemental Figure S2, Supporting Information), precluding an increased browning of WAT cells. Oleic acid has, among fatty acids and especially saturated ones such as palmitic acid, the highest thermogenic capacity.^[30,31] As both the HFD and HFHFr interventions increased the synthesis of oleic acid, at least in liver tissues, as a consequence of the desaturation of dietary stearic acid,^[13] this effect could partly explain the induction of BAT-related thermogenesis markers produced by both dietary interventions. Moreover, HFHFr diet induced hyperleptinemia when compared to the HFD (x1.6 vs HFD, see Figure 3A2). As the effects of leptin on the central nervous system translate into reduced solid food intake and increased thermogenesis,^[32] the difference in circulating leptin could explain: i) the reduced intake of solid chow observed in the HFHFr rats, as reflected by a significant reduction in ingested solid calories (data not shown), and (ii) the fact that the HFHFr rats, although showing a significant greater increase in total calorie consumption than the HFD rats (x1.30 vs HFD, see Figure 1A), also managed to keep their body weight under control.

After 3 months of the dietary intervention, the HFD enriched in stearic acid and without exogenous cholesterol induced fatty

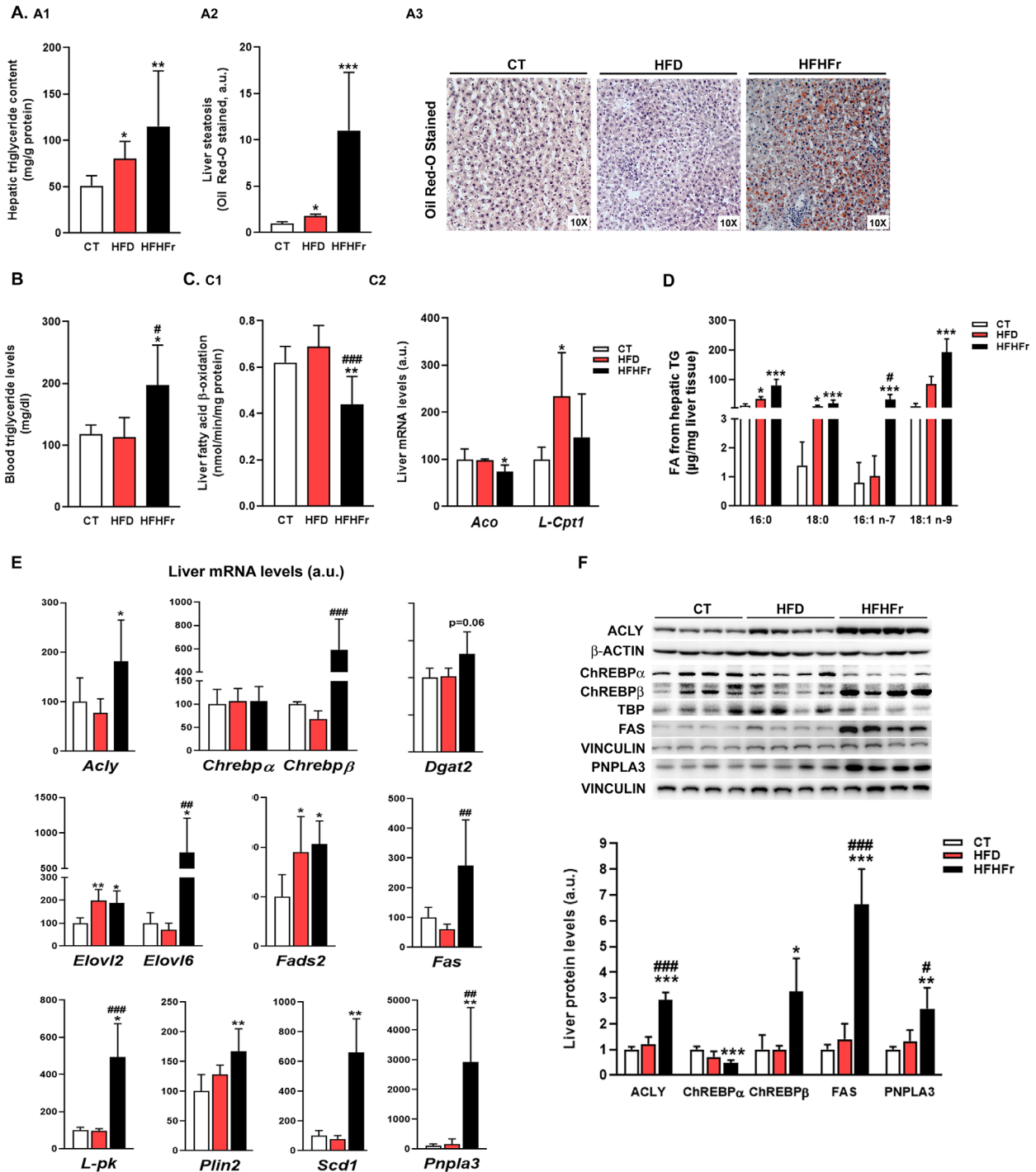


Figure 5. Effects of HFD and HFHF on liver steatosis, blood triglycerides, and liver markers of DNL. A) Bar plots showing the content of triglycerides as mg/g of liver protein and arbitrary units (a.u.) of Oil-Red O staining of liver samples from CT, HFD and HFHF rats. Oil-Red O representative stained liver samples for each experimental condition are shown in the right part of the figure. B) Bar plot showing blood levels of triglycerides of CT, HFD, and HFHF rats. C) Bar plots showing fatty acid β -oxidation activity and the relative mRNA levels of *Aco*, and *L-Cpt1* genes of liver samples from CT, HFD, and HFHF rats. D) Bar plots showing the concentration of palmitic (16:0), stearic (18:0), palmitoleic (16:1 n-7), and oleic (18:1 n-9) acids present in liver triglycerides from CT, HFD, and HFHF rats. E) Bar plots showing the relative mRNA levels of *Acly*, *Chrebp α* and β , *Chop*, *Dgat2*, *Elov12* and *6*, *Fads2*, *Fas*, *L-pk*, *Plin2*, *Scd1*, and *Pnpla3* genes of liver samples from CT, HFD, and HFHF rats. F) Bar plots showing the content of ACLY, ChREBP α and β , FAS, and PNPLA3 proteins in the liver tissue obtained from CT, HFD, and HFHF rats; in the upper part of the figure, representative WB bands corresponding to the three different study groups are shown. Each bar represents the mean \pm SD of 7–8 different samples; for WB analysis, we used four different pooled samples for each experimental condition, each pool was obtained from mixing equal amounts of two individual tissue samples. *** $p < 0.001$, ** $p < 0.01$, * $p < 0.05$ versus CT; ### $p < 0.001$, ## $p < 0.01$, # $p < 0.05$ versus HFD.

liver accretion without promoting clear signs of liver inflammation and oxidative stress. However, the degree of fatty liver attained was very mild and there were no changes in the triglyceridemia and glucose homeostasis parameters, although an early manifestation of liver insulin resistance was detected in the form of an increased expression of the key gluconeogenic enzyme, PEPCK, and in the accretion of ceramides in liver (see Figure 3F3 and C, respectively). This suggests that in order to obtain a fully developed, liver-centered, metabolic disturbance solely with the HFD, feeding periods longer than three months should be used.

This situation was completely changed when liquid fructose supplementation was added to the HFD. Liquid fructose supplementation increased hepatic DNL and decreased fatty acid oxidation by increasing and decreasing, respectively, the activity of two transcription factors, ChREBP and Peroxisome proliferator activated receptor α (PPAR α), whose fructose-related effects have been described previously by work of our research group and others.^[9,25,26] These combined effects, together with the flux of dietary fatty acids provided by the solid HFD, were probably responsible for the huge increase in liver TG deposition observed in the HFHFr rats with respect to the HFD rats. Importantly, the development of fatty liver by liquid fructose supplementation was not associated with any manifestation of liver inflammation or increased oxidative stress. We have previously shown in rat and murine models that up to a 15% w/w solution of liquid fructose does not modify plasma endotoxin or lipopolysaccharide-binding protein levels,^[10,33] which are markers of alterations in the intestinal barrier permeability and an increased flux of pro-inflammatory bacterial endotoxins to the liver.^[34,35]

The marked accretion of liver TG observed in the HFHFr rats occurred despite the presence of hypertriglyceridemia, which suggests that some of the newly synthesized fatty acids had been incorporated into VLDL-TG and drained into the blood. The HFD rats did not show hypertriglyceridemia, indicating that dietary fatty acids probably do not affect the liver output of VLDL. Thus, the HFHFr diet not only resulted in fatty liver, but also in a clear hypertriglyceridemia, which, again, seems to be related to the effects of fructose decreasing liver PPAR α and increasing ChREBP transcriptional activities. It is well known that drugs like fibrates, ligands and activators of PPAR α , reduce VLDL production and increase its catabolism in the vasculature, thus effectively reducing hypertriglyceridemia.^[36,37] Moreover, the gene encoding the PNAPL3 protein, whose lipase activity facilitates the transfer of fatty acids trapped in liver vesicles for re-synthesis into TG incorporated into VLDLs,^[28] is under the transcriptional control of ChREBP.^[27] This fructose-mediated promotion of liver VLDL production could explain also the selective increased levels of phosphorylated IRE-1 detected exclusively in the liver samples of HFHFr rats, without eliciting a full unfolded protein response. Although the precise molecular mechanism involved it is not well defined at present, other studies^[38–40] have consistently shown that IRE-1 activity is directly involved in the production of liver VLDL. However, in our model, the increased exportation of VLDL-TG to the blood did not prevent the manifestation of fatty liver.

Related to the different main fate of de novo versus dietary fatty acids (exportation to the whole organism in the form of VLDL, or packed and stored in the form of liver TG deposits, respectively) is the marked difference in the accumulation of liver Cer

and DAG between the HFD and HFHFr groups. While the flux of dietary saturated fatty acids provided by the HFD resulted in an increased accretion of liver Cer, the fructose-related increase in DNL resulted in an almost normalization of the content of liver Cer with regard to control values, while the liver content of several DAG species increased sharply, especially those containing palmitic, palmitoleic and oleic acids, markers of DNL. Again, the increase in DAG species containing palmitic acid in the livers of HFHFr rats points to an increased de novo synthesis of this fatty acid, as those same DAG species were not significantly modified in the livers of HFD rats, which obtained palmitic acid mainly from a dietary origin. DGAT is the last enzyme involved in the synthesis of TG, incorporating the third fatty acyl chain into a preformed diacylglycerol molecule. Of the two isoforms of DGAT expressed in the liver, DAGT1 and DGAT2, DGAT2 seems to preferentially use de novo synthesized fatty acids, forming TG that are packed into newly formed VLDLs for exportation.^[41,42] We detected a marginally significant increase in the expression of DAGT2 in the livers of HFHFr rats, indicating that the increased amount of newly formed fatty acids is not matched with a corresponding increase in DGAT2 expression/activity, which could be responsible for the increased accretion of DAG species in the livers of fructose-supplemented rats.

Despite the increase in liver DAG content, fructose-supplemented rats did not show a clear state of liver insulin resistance, presenting a marked reduction in the expression of liver PEPCK protein, a key enzyme controlling liver gluconeogenic activity. Very recently, Smith et al. showed that an increase in β -oxidation in skeletal muscle is related to manifestations of glucose intolerance.^[43] Thus, in our experimental setting, the mild changes detected in glucose homeostasis, with a reduced ISI value in the HFHFr rats, could be attributed, at least partly, to the increased flux of liver TG to the skeletal muscle, promoting a shift in the energy substrate use from glucose to fatty acids in these animals. Although we did not analyze the effects of the different dietary interventions on the lipid content and composition of skeletal muscle, our data indicated that, at least for the HFHFr rats, possible alterations in glucose homeostasis resulting in insulin resistance originate from the liver.

Overall, our model recreates the first manifestation in NAFLD development, fatty liver, originated basically from dietary factors. In our setting, fatty liver derives from a direct alteration of liver lipid metabolism, without the influence of other metabolic disturbances, such as obesity, inflammation or type 2 diabetes. Moreover, fatty liver develops together with hypertriglyceridemia also of hepatic origin, a dyslipidemia that is often associated to NAFLD. As fatty liver, contrary to NASH, can be easily reverted, this model can be useful in the search of effective pharmacological therapies for the early stages of NAFLD

In conclusion by combining a solid chow devoid of free cholesterol and rich in saturated fatty acids (palmitic and stearic acid) with liquid fructose supplementation (10 % w/w), we characterized in female Sprague-Dawley rats a dietary model of fatty liver with hypertriglyceridemia that had no manifestations of liver inflammation or oxidative stress. Moreover, in this model, changes in liver metabolism were not accompanied by an increased accretion of WAT and body weight, with a minimal effect on whole body insulin sensitivity. Furthermore, our data clearly

demonstrated that increased DNL and reduced fatty acid catabolism, two fructose-related liver metabolic alterations, were necessary for the rapid manifestation of liver steatosis. Moreover, the activation of ChREBP was responsible not only for the increased DNL, but also for the appearance of hypertriglyceridemia, probably mediated by the increased expression of PNPLA3, a lipase that mobilizes monounsaturated-enriched TG stored in lipid droplets for VLDL formation and secretion.

4. Experimental Section

Animals: Two-month-old female Sprague Dawley rats (Envigo, Barcelona, Spain) were housed two per cage under conditions of constant humidity (40–60%) and temperature (20–24 °C), with a light/dark cycle of 12 h. Twenty-four female rats were randomly assigned to three groups ($n = 8$ in each) and fed ad libitum for 3 months. Female rats were used because we have previously shown that they are more sensitive to the deleterious effects of fructose on glucose homeostasis than male rats.^[8] The control group (CT) was fed regular chow diet (2018 Teklad Global, 18% of provided calories as fat), whereas the high-fat diet group (HFD) was fed an HFD (Teklad Custom Diet TD. 180456, 46.9% of provided calories as fat, of which 21% w/w is cocoa butter containing 25% of palmitic acid and 35% of stearic acid). The composition of the two diets is shown in the Supplementary Material (Table S1, Supporting Information). Both groups had free access to water. Finally, the high-fat-high-fructose group (HFHFr) was fed HFD and had free access to a 10% w/v fructose solution as the drinking beverage. In the CT group, one rat was euthanized before the end of the experimental period, due to a growing tumor; thus, the final n for the CT group was 7. All experiments were performed under the principles and procedures outlined in the guidelines established by the Bioethics Committee of the University of Barcelona (Autonomous Government of Catalonia Act 5/21 July 1995). The Animal Experimentation Ethics Committee of the University of Barcelona approved all the experimental procedures involving animals (approval no. 10 106).

Oral Glucose Tolerance Test: An oral glucose tolerance test (OGTT) was performed in the last week of the treatment as described previously.^[17] Glucose levels were determined in all the blood samples using a handheld glucometer (Accutrend Plus System, Cobas, Roche Farma, Barcelona, Spain). Serum was obtained from blood samples collected at 0, 15, and 120 min, and insulin levels were measured using a rat insulin enzyme-linked immunosorbent assay (ELISA) kit (Millipore, Billerica, MA, USA).

Sample Preparation: At the end of the treatment, rats were fasted for 2 h and blood samples were obtained from the tail vein to measure TG, cholesterol, and glucose levels, using an Accutrend Plus system glucometer (Cobas, Roche Farma, Barcelona, Spain). The rats were then immediately anesthetized with ketamine/xylazine (9 mg 40 μg^{-1} per 100 g of body weight, respectively) and blood was collected into micro-tubes (Sarstedt AG & Co., Nümbrecht, Germany) through cardiac puncture and centrifuged at 10 000 $\times g$ for 5 min at room temperature. Rats were euthanized by exsanguination, and the liver, muscle, interscapular brown adipose tissue (BAT), subcutaneous and perigonadal white adipose tissue (sWAT and pWAT, respectively), were excised and weighed. For the histological studies, samples of the liver from each animal were fixed overnight in 10% neutral buffered formalin solution or were embedded in OCT and frozen quickly in liquid nitrogen and stored at -80 °C. The remaining liver tissues were perfused, immediately frozen in liquid nitrogen, and stored at -80 °C until use.

Serum Analysis: Serum adiponectin, insulin, and leptin concentrations were determined using specific ELISA kits (EZRADP-62K; EZRMI-13K; EZRL-83K, respectively) from Millipore (Billerica, MA, USA). The non-esterified free fatty acids (NEFA) colorimetric kit was from BioScientific (Austin, TX, USA) and the kits for alanine (ALT) and aspartate aminotransferase (AST) kinetics were from SpinReact (Girona, Spain). The insulin sensitivity index (ISI) was calculated as $2 / [\text{insulin (nM)} \times \text{blood glucose } (\mu\text{M}) + 1]$.^[44]

Liver Lipid Content: Hepatic TG and cholesterol were extracted as described by Qu et al.^[44] and determined using a colorimetric assay kit (Ref: 41 030 and MD41021, respectively) from Spinreact (Girona, Spain).

Histological Studies: Paraffin-embedded liver sections were cut to 5 μm and stained with hematoxylin and eosin to assess the degree of necrosis. Lipid accumulation was analyzed in OCT-embedded liver sections stained with Oil-Red O (ORO). Images were acquired with a Leica DMSL microscope equipped with a DP72 camera (Leica Microsystems, Barcelona, Spain) and analyzed using Image J 1.49 software (National Institutes of Health, Bethesda, MD, USA). The area of positive ORO staining was calculated as the positively stained area per total area. All procedures were carried out in the Animal Histopathology Laboratory at the University of Barcelona.

Lipidomic Analysis in Rat Liver Homogenates: Fatty acid methyl esters from liver TG were determined by gas chromatography/electron ionization mass spectrometry as described previously.^[17] Levels of diacylglycerols (DAG), and ceramides (Cer) in rat livers were determined by liquid chromatography-tandem mass spectrometry (LC-MS/MS) system as described previously.^[17]

Fatty Acid β -oxidation: Total fatty acid β -oxidation was determined in rat livers and muscle, as described by Lazarow,^[45] using 30 μg of post-nuclear supernatant from the liver samples and 40 μg from the muscle samples.

RNA Preparation and Analysis: Total RNA was isolated from different tissues by using the Trisure reagent (Bioline, Meridian Biosciences, Cincinnati, OH, USA) according to the manufacturer's instructions. RNA concentration was determined by measuring absorbance at 260 nm, while the 260/280 nm absorbance ratio was used to analyse RNA quality. Real-time polymerase chain reaction (RT-qPCR) was performed as described previously.^[11] The TATA box-binding protein (tbp) was used as the house-keeping gene to normalize the results. The primer sequences, Genbank TM number, and PCR product lengths are listed in the Supplementary Material (Table S2, Supporting Information).

Protein Preparation and Western Blot Analysis: Tissue samples and western blot analysis were prepared and performed as described previously.^[11] Western blots were performed using four samples per group, each sample pooled from two animals. A total of 30 μg of protein extracts (10 μg for PNPLA3 determination) was used. Protein concentrations were determined by the Bradford method.^[46] To confirm the uniformity of protein loading, blots were incubated with anti- β -actin, or anti- β -tubulin antibodies (Sigma-Aldrich, St. Louis, MO, USA) or anti-vinculin antibody (Santa Cruz Biotech, Dallas, TX, USA), as a control for total protein extracts, and with anti-TBP antibody (AbCam, Cambridge, UK), as a control for nuclear protein extracts. A list of antibodies used in western blot analysis is shown in the Supplementary Material (Table S3, Supporting Information).

Statistical Analysis: Results are expressed as mean \pm standard deviation (SD). Significant differences were established by one-way ANOVA and Šidák's post-hoc test for selected comparisons (GraphPad Software version 8, San Diego, CA, USA). When the SD of the groups was different according to Bartlett's test, the data were transformed into their logarithms and ANOVA was rerun, or the corresponding non-parametric test was applied. The OGTT curves for glucose and insulin were analyzed by two-way ANOVA. The level of statistical significance was set at $p < 0.05$.

Supporting Information

Supporting Information is available from the Wiley Online Library or from the author.

Acknowledgements

This research was funded Grant SAF2017-82369-R funded by MCIN/AEI/10.13039/501100011033 and by ERDF A way of making Europe, Generalitat de Catalunya (2017 SGR 38). A.M.V. is a predoctoral fellow, BECAL grant program BCAL04-327, from the Government of Paraguay. A.S.-V. is

recipient of the Instituto de Salud Carlos III Miguel Servet fellowship (grant CP II 17/00029).

The authors thank the University of Barcelona's Language Advisory Service for revising the manuscript.

Conflict of Interest

The authors declare no conflict of interest.

Author Contributions

N.R. and J.C.L. contributed equally to this work. A.M.V. and N.R. were in charge of all experiments and prepared the figures; R.B. and M.G. contributed to the PCR/Western blot experiments; A.S.-V. and I.L. performed FAME analysis; J.R.-M. performed lipidomic analysis; R.M.S. helped in data interpretation and reviewed the manuscript; J.C.L. and M.A. designed and supervised the experiments, analyzed the data, and reviewed the manuscript; J.C.L. wrote the manuscript. All authors have read and agreed to the published version of the manuscript.

Data Availability Statement

The data that support the findings of this study are available from the corresponding author upon reasonable request.

Keywords

ceramides, diacylglycerols, fatty acid β -oxidation, lipidomics, liver steatosis, NAFLD

Received: December 9, 2021

Revised: January 18, 2022

Published online:

- [1] N. Than, P. N. Newsome, *Atherosclerosis* **2015**, 239, 192.
- [2] G. A. Kim, H. C. Lee, J. Choe, M. J. Kim, M. J. Lee, H. S. Chang, I. Y. Bae, H. K. Kim, J. An, J. H. Shim, K. M. Kim, Y. Lim, *J. Hepatol.* **2018**, 68, 140.
- [3] N. N. El-Agroudy, A. Kurzbach, R. N. Rodionov, J. O'Sullivan, M. Roden, A. L. Birkenfeld, D. H. Pesta, *Trends Endocrinol. Metab.* **2019**, 30, 701.
- [4] N. Pydyn, K. Miękus, J. Jura, J. Kotlinowski, *Pharmacol. Reports* **2020**, 72, 1.
- [5] M. V. Chakravarthy, T. Waddell, R. Banerjee, N. Guess, *Gastroenterol. Clin. North Am.* **2020**, 49, 63.
- [6] P. K. Santhekadur, D. P. Kumar, A. J. Sanyal, *J. Hepatol.* **2018**, 68, 230.
- [7] T. Coll, X. Palomer, F. Blanco-Vaca, J. C. Escolà-Gil, J. C. Escolà-Gil, R. M. Sánchez, J. C. Laguna, M. Vázquez-Carrera, *Endocrinology* **2010**, 151, 537.
- [8] L. Vilà, N. Roglans, V. Perna, R. M. Sánchez, M. Vázquez-Carrera, M. Alegret, J. C. Laguna, *J. Nutr. Biochem.* **2011**, 22, 741.
- [9] A. Rebollo, N. Roglans, M. Baena, R. M. Sánchez, R. M. Sánchez, M. Vázquez-Carrera, J. C. Laguna, *Biochim. Biophys. Acta - Mol. Cell Biol. Lipids* **2014**, 1841, 514.
- [10] M. Baena, G. Sangüesa, A. Dávalos, M.-J. E. Latasa, A. Sala-Vila, R. M. Sánchez, N. Roglans, J. C. Laguna, M. Alegret, *Sci. Rep.* **2016**, 6, 26149.
- [11] G. Sangüesa, N. Roglans, J. C. Montañés, M. Baena, A. M. Velázquez, R. M. Sánchez, M. Alegret, J. C. Laguna, *Mol. Nutr. Food Res.* **2018**, 62, 1800777.
- [12] G. Sangüesa, J. C. Montañés, M. Baena, R. M. Sánchez, N. Roglans, M. Alegret, J. C. Laguna, *Eur. J. Nutr.* **2019**, 58, 1283.
- [13] L. Hodson, B. A. Fielding, *Prog. Lipid Res.* **2013**, 52, 15.
- [14] J. Rodríguez-Morató, J. Galluccio, G. G. Dolnikowski, A. H. Lichtenstein, N. R. Matthan, *Arterioscler. Thromb. Vasc. Biol.* **2020**, 2953.
- [15] T. Coll, E. Eyre, R. Rodríguez-Calvo, X. E. Palomer, R. M. Sánchez, M. Merlos, J. C. Laguna, M. Vázquez-Carrera, *J. Biol. Chem.* **2008**, 283.
- [16] K. Wouters, P. J. van Gorp, V. Bieghs, M. J. Gijbels, H. Duimel, D. Lütjohann, A. Kerksiek, R. van Kruchten, N. Maeda, B. Staels, M. van Bilsen, R. Shiri-Sverdlov, M. H. Hofker, *Hepatology* **2008**, 48, 474.
- [17] A. M. Velázquez, N. Roglans, R. Bentanachs, M. Gené, A. Sala-Vila, I. Lázaro, J. Rodríguez-Morató, R. M. Sánchez, J. C. Laguna, M. Alegret, *Nutrients* **2020**, 12, 3240.
- [18] H. Zhou, C. J. Urso, V. Jadeja, *J. Inflamm. Res.* **2020**, 13, 1.
- [19] H. Wang, R. Q. Sun, X. Y. Zeng, X. Zhou, S. Li, E. Jo, J. C. Molero, J. M. Ye, *Endocrinology* **2015**, 156, 169.
- [20] R. J. Perry, V. T. Samuel, K. F. Petersen, G. I. Shulman, *Nature* **2014**, 510, 84.
- [21] V. T. Samuel, G. I. Shulman, *N. Engl. J. Med.* **2019**, 381, 1866.
- [22] M. C. Renton, S. L. McGee, K. F. Howlett, *Obes. Rev.* **2020**, 1.
- [23] V. T. Samuel, G. I. Shulman, *Cell Metab.* **2018**, 27, 22.
- [24] K. Sakamoto, G. D. Holman, *Am. J. Physiol. Endocrinol. Metab.* **2008**, 295, E29.
- [25] N. Roglans, L. Vilà, M. Farré, M. Alegret, R. M. Sánchez, M. Vázquez-Carrera, J. C. Laguna, *Hepatology* **2007**, 45.
- [26] F. Baraille, J. Planchais, R. Dentin, S. Guilmeau, C. Postic, *Physiology (Bethesda)* **2015**, 30, 428.
- [27] C. Dubuquoy, C. Robichon, F. Lasnier, C. Langlois, I. Dugail, F. Foufelle, J. Girard, A. F. Burnol, C. Postic, M. Moldes, *J. Hepatol.* **2011**, 55, 145.
- [28] P. Pingitore, S. Romeo, *Biochim. Biophys. Acta Mol. Cell Biol. Lipids* **2019**, 1864, 900.
- [29] N. J. Rothwell, M. J. Stock, *Nature* **1979**, 281, 31.
- [30] S. Krishnan, J. A. Cooper, *Eur. J. Nutr.* **2014**, 53, 691.
- [31] S. Shin, K. M. Ajuwon, *Nutrients* **2018**, 10.
- [32] Y. H. Tseng, A. M. Cypess, C. R. Kahn, *Nat. Rev. Drug Discovery* **2010**, 9, 465.
- [33] G. Sangüesa, M. Baena, N. Hutter, J. C. Montañés, R. M. Sánchez, N. Roglans, J. C. Laguna, M. Alegret, *Nutrients* **2017**, 9.
- [34] I. Bergheim, S. Weber, M. Vos, S. Krämer, V. Volynets, S. Kaserouni, C. J. McClain, S. C. Bischoff, *J. Hepatol.* **2008**, 48, 983.
- [35] A. Spruss, G. Kanuri, S. Wagnerberger, S. Haub, S. C. Bischoff, I. Bergheim, *Hepatology* **2009**, 50, 1094.
- [36] N. Bougarne, B. Weyers, S. J. Desmet, J. Deckers, D. W. Ray, B. Staels, K. De Bosscher, *Endocr. Rev.* **2018**, 39, 760.
- [37] J. C. Fruchart, M. P. Hermans, J. Fruchart-Najib, T. Kodama, *Curr. Atheroscler. Rep.* **2021**, 23.
- [38] A. H. Lee, E. F. Scapa, D. E. Cohen, L. H. Glimcher, *Science* **2008**, 320, 1492.
- [39] S. Wang, Z. Chen, V. Lam, J. Han, J. Hassler, B. N. Finck, N. O. Davidson, R. J. Kaufman, *Cell Metab.* **2012**, 16, 473.
- [40] K. Zhang, S. Wang, J. Malhotra, J. R. Hassler, S. H. Back, G. Wang, L. Chang, W. Xu, H. Miao, R. Leonardi, Y. E. Chen, S. Jackowski, R. J. Kaufman, *EMBO J.* **2011**, 30, 1357.
- [41] V. A. Zammit, *Biochem. J.* **2013**, 451, 1.
- [42] B. Bhatt-Wessel, T. W. Jordan, J. H. Miller, L. Peng, *Arch. Biochem. Biophys.* **2018**, 655, 1.
- [43] C. D. Smith, C. T.e Lin, S. L. McMillin, L. A. Weyrauch, C. A. Schmidt, C. A. Smith, I. J. Kurland, C. A. Witczak, P. D. Neuffer, *Am. J. Physiol. - Endocrinol. Metab.* **2021**, 320, E938.
- [44] S. Qu, D. Su, J. Altomonte, A. Kamagate, J. He, G. Perdomo, T. Tse, Y. Jiang, H. H. Dong, *Am. J. Physiol. Endocrinol. Metab.* **2007**, 292, E421.
- [45] P. Lazarow, *Methods Enzymol* **1981**, 72, 315.
- [46] M. Bradford, *Anal. Biochem.* **1976**, 72, 248.